

An Interferometric Microwave Comb Generator

R. Kimberk, C. E. Tong, H. Gibson, R. W. Wilson, R. Blundell, S. Paine, and T. R. Hunter
Smithsonian Astrophysical Observatory
60, Garden Street, Cambridge, MA02138, USA

Abstract

We have developed a scheme for generating a comb of radio frequencies, covering the microwave to millimeter spectral range. The system utilizes a single diode laser coupled to an optical interferometer and photodetector. Frequency modulating the laser at a rate of 2.154 GHz, we observe an electrical signal from the photodetector with a spectrum that is a comb that extends beyond the 40th harmonic of the fundamental modulation frequency. The line width of the electrical output is less than 2 Hz. We have compared the phase stability of an element of the comb with the output from a classical diode frequency multiplier (both driven from the same source) and have concluded that a phase-stable output can be generated. Finally, we have developed analytical and numerical models that suggest that our scheme may be used for frequency generation through the submillimeter.

Introduction

The design of photonic local oscillators for use with low noise heterodyne receiver systems has been motivated by the development of photo detectors with frequency response in the microwave and millimeter ^{1,2}. Attempts at producing a usable photonic local oscillator are usually based on the mixing of the outputs of two solid-state lasers in a photo detector. The poor line width and frequency stability of the simple heterodyne systems have led to more complex systems to control the phase and frequency of the resulting tone ^{3,4}. We have developed a single laser homodyne system. The operating principle is similar to the time delay / phase shift frequency discriminator used to demodulate frequency and phase modulated radio signals ⁵. An angle modulated (either frequency or phase modulated) signal is demodulated and converted to an amplitude-modulated signal, through the use of an appropriate differentiator. In our device we incorporate a time delay frequency discriminator (interferometer) with the time delay set to recover a maximum number of harmonics of the modulation signal. The HP 11980A fiber optic interferometer is based on comparable techniques and other similar schemes have been used to measure laser chirp ^{6,7}.

System description

The optical output frequency of a semiconductor diode laser is a function of its bias current. Modulating the bias current produces an angle modulated optical signal. In our scheme the sum of a DC bias and a microwave signal is used to set the operating point and modulate the optical output frequency of a Fabry-Perot laser diode. The diode is an SDL-5432 with a nominal output wavelength of 830 nm. The wavelength change is about 0.01 nm/mA, which is equivalent to a

frequency shift of about 4 GHz/mA. The DC bias current is set sufficiently above the threshold value for lasing to occur, so that at no time does the sum of the DC and microwave current fall below threshold. The angle modulated optical signal from the laser passes through an optical isolator and then is coupled to the input of a Mach-Zehnder interferometer. The interferometer is constructed from two Newport, F-CPL-S22855, 3 dB single mode fiber couplers. The first of these is used to split the laser output into two equal power components, one of these incurs an additional path length delay, δ , resulting in a time delay $\Delta t = \delta/c\sqrt{\epsilon_r}$ before being recombined with the other at the output of the second coupler. Figure 1 is a diagram of this system.

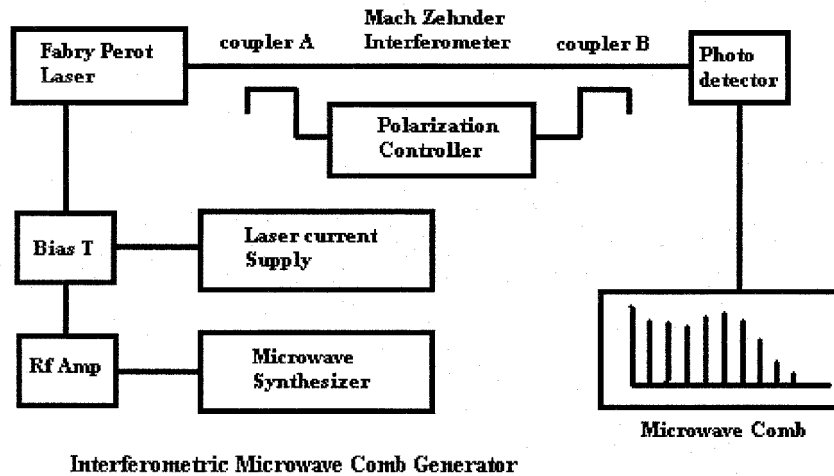


Figure 1. The system diagram

The time domain description of the angle modulated laser output may be written:

$$a(t) = \cos [\omega_c t + \beta \sin \omega_m t] \quad (1)$$

where ω_c is the carrier or optical frequency, ω_m is the modulation frequency, and β is the modulation index (the amplitude of $\sin \omega_m t$). β is equal, for the particular case of frequency modulation, to $\Delta\omega_c/\omega_m$: the maximum change in carrier frequency, $\Delta\omega_c$, divided by the modulating frequency, ω_m .

At the interferometer output we therefore have:

$$a_1(t) = A \cos [\omega_c t + \beta \sin \omega_m t] \quad (2)$$

and the delayed signal

$$a_2(t) = A \cos [\omega_c(t - \Delta t) + \beta \sin \omega_m(t - \Delta t)] \quad (3)$$

Setting the time delay equal to one half of the period of the modulating frequency, $\Delta t = \pi/\omega_m$, in order to maximize the resulting comb bandwidth, we have

$$a_2(t) = A \cos [(\omega_c t - \pi\omega_c/\omega_m) - \beta \sin \omega_m t] \quad (4)$$

The sum of expressions (2) and (4) may be written

$$a_1(t) + a_2(t) = 2A \cos(\beta \sin \omega_m t + \phi) \cos(\omega_c t - \phi) \quad (5)$$

where $\phi = \pi\omega_c/2\omega_m$

The output of the interferometer consists of an optical carrier

$$\cos(\omega_c t - \phi) \quad (6)$$

with a low frequency amplitude envelope given by

$$2A \cos(\beta \sin \omega_m t + \phi) \quad (7)$$

In equations (4) and (5) the bandwidth of the amplitude modulation is also maximized for additional delays of $2n\pi/\omega_m$ for $n = 1, 2, 3 \dots$. In addition, to achieve the output described by expression (5), the two signals must also have the same polarization. A polarization controller is therefore placed in one arm of the interferometer and manually adjusted to maximize the interferometer output.

The interferometer output is coupled to a photodetector that produces an electrical signal whose amplitude is proportional to the square of the amplitude envelope, expression (7). The voltage output at the photodetector may be written:

$$\begin{aligned} V_{\text{out}} &= k A \cos^2 (\beta \sin \omega_m t + \phi) \\ &= k A [1 + \cos(2\beta \sin \omega_m t + 2\phi)] \end{aligned} \quad (8)$$

where k is a constant related to the effective responsivity of the detector. In this study, the photodetector used was a New Focus model 1434. A 1 mW input at 1.06 μm produced an output power of -37 dBm from near DC to 25 GHz.

Examination of expression (8) shows that the action of the square law photodetector not only shifts the angle modulated optical spectrum to base band, but also generates a modulation index of 2β , twice the original index of expression (1). In the frequency domain, expression (8) is a comb of spectral lines separated by ω_m . Expression (8) can be expanded into a series

$$V_{\text{out}} = k A \left[1 + \sum_{n=-\infty}^{+\infty} J_n(2\beta) \cos (n\omega_m t + 2\phi) \right] \quad (9)$$

where $J_n(x)$ is the Bessel function of the first kind, of order n . As the modulation index is increased, the power is shared with more and more sidebands and the bandwidth of the signal increases. According to Carson's rule⁵, 98% of this power is contained within a bandwidth of

$$(2\beta + 1)\omega_m \quad (10)$$

As an example, modulating our laser (with a modulation sensitivity of 0.01 nm/mA, or 4 GHz/mA) to a depth of 10 mA at a frequency of 10 GHz, yields $\beta = \Delta\omega_c/\omega_m = 4$, so the bandwidth of the microwave comb, given by expression (10), is 90 GHz.

Output Noise Power

The interferometric comb generator takes advantage of the temporal coherence of the laser to produce a more spectrally pure output than is possible with a heterodyne (two laser) mixing scheme. The temporal coherence of the laser is related to its line width and power spectral density. The line width specification frequently given by the laser manufacturer is the wavelength between the Fabry-Perot modes that are 3 dB below the dominant mode. This specification should not be confused with the line width (FWHM), $\delta\omega$, of any given mode, which is of order 0.1 MHz⁹. The power spectral density of a given mode has a Lorentzian distribution, parameterized by the center frequency and $\delta\omega$ of about 6×10^5 radian/s.

The intrinsic laser phase noise may be modeled as a random phase modulation of the optical carrier⁸. We implement this in our model by introducing a phase term, $\beta_n \sin \omega_n t$, that modulates the optical carrier.

$$a(t) = \cos [\omega_c t + \beta_n \sin \omega_n t] \quad (11)$$

The absolute value of the noise frequency ω_n can assume any value from zero up to a few times $\delta\omega$. Its mean value is $\delta\omega/2$. For a well behaved laser, the noise modulation index β_n , should be small ($\beta_n < 1$) and is a Lorentzian function of ω_n .

Equation (11) can be expanded in a series of Bessel functions:

$$a(t) = \sum_p J_p(\beta_n) \cos (p\omega_n t + \omega_c t) \quad (12)$$

Since β_n is small, we retain only the linear terms of the series

$$a(t) = \cos \omega_c t + \beta_n \cos (\omega_n t + \omega_c t) \quad (13)$$

Expression (13) implies that the noise power density at an offset ω_n from the optical carrier is β_n^2 . Next, we investigate the effect of the extra phase noise term in the entire system. The analysis given in the previous section is repeated with the addition of the phase noise term:

$$a(t) = \cos(\omega_c t + \beta \sin \omega_m t + \beta_n \sin \omega_n t) \quad (14)$$

The interferometer output can be written as

$$a_1(t) + a_2(t) = 2A \cos[\beta \sin \omega_m t + \phi + \beta_n/2 (\sin \omega_n t - \sin \omega_n(t - \Delta t))] \cos[\omega_c t - \phi + \beta_n/2 (\sin \omega_n t + \sin \omega_n(t - \Delta t))] \quad (15)$$

The photodetector extracts the amplitude envelope of the interferometer output to yield

$$V_{out} = kA \cos^2[(\beta \sin \omega_m t + \phi + \beta_n/2 (\sin \omega_n t + \sin \omega_n(t - \Delta t)))] \quad (16)$$

For a path length difference of 100 mm Δt will be equal to 5×10^{-10} s. Then $\delta\omega\Delta t$ will be about 3×10^{-4} and the product $\omega_n\Delta t \ll 1$. In the limit of small argument, $\cos(\omega_n\Delta t) \sim 1$ and $\sin(\omega_n\Delta t) \sim \omega_n\Delta t$ so that

$$[\sin \omega_n t + \sin \omega_n(t - \Delta t)] \sim \omega_n\Delta t \cos \omega_n t \quad (17)$$

V_{out} (expression (16)) can then be rewritten as

$$V_{out} = kA \cos^2(\beta \sin \omega_m t + \phi + \beta_n/2 (\omega_n\Delta t \cos \omega_n t)) = .5 kA + 1/2 kA \cos(2\beta \sin \omega_m t + 2\phi + \beta_n \omega_n\Delta t \cos \omega_n t) \quad (18)$$

the AC component of V_{out} may be expanded using a Jacobi – Anger series

$$\sum_{p=-\infty}^{+\infty} \sum_{k=-\infty}^{+\infty} J_p(2\beta) J_k(\beta_n \omega_n\Delta t) \cos[2\phi + p\omega_m t + k(\omega_n t + \pi/2)] \quad (19)$$

Since $\beta_n \omega_n\Delta t$ is small, we retain only the lowest orders of the series, i.e. $k = -1, 0, \text{ and } 1$.

$$V_{out} = \sum_{p=-\infty}^{+\infty} \sum_{k=-\infty}^{+\infty} J_p(2\beta) [\cos(p\omega_m t + 2\phi) + (\beta_n \omega_n\Delta t) \cos(p\omega_m t + 2\phi + \omega_n t + \pi/2) - (\beta_n \omega_n\Delta t) \cos(p\omega_m t + 2\phi - \omega_n t - \pi/2)] \quad (20)$$

From the above expression we can say that associated with each discrete line in the comb of the photodetector output there is a noise sideband of power density $(\beta_n \omega_n\Delta t)^2$ at an offset of ω_n . Comparing this noise power density to that of the intrinsic laser noise given by equation (13), we note that the noise power density is reduced by a factor of $(\omega_n\Delta t)^2$.

At the mean offset of ω_n , equal to $\delta\omega/2$, the noise reduction is simply $(\delta\omega\Delta t/2)^2$. As $\delta\omega/2$ is equal to $1/\tau$, where τ is the coherence time of the laser, $(\delta\omega\Delta t/2)^2 = (\Delta t/\tau)^2$. The same result may be derived from the normalized autocorrelation function, referred to as the degree of temporal coherence.

For example, in our experiment the path length difference was set at 140 mm, which is equivalent to a path length delay of 7×10^{-10} s in glass fiber. For $\delta\omega$ of about 3×10^5 rad/s, we have

$$(\delta\omega\Delta t/2)^2 = ((7 \times 10^{-10}) \times (3 \times 10^5) / 2)^2 \sim 10^{-8} \quad (21)$$

The noise power of the photodetector output is improved compared to that of the original laser output by about 80 dB.

Measured values of noise power for a comb line at 10.77 GHz are; - 80 dBc/Hz at 1 kHz offset, - 80 dBc/Hz at 10kHz, -100 dBc/Hz at 100kHz, and -110 dBc/Hz at 1 MHz. The shape of the noise pedestal of the comb matched the shape of the noise pedestal of the modulating signal. This suggests that the measured noise was predominately the noise of the modulating signal and not the laser phase noise.

Numerical Model

A numerical model has been developed to provide a theoretical framework through which a detailed understanding of the effect that various parameters, such as carrier frequency, modulation rate and index, phase relationship between carrier and modulating signal, dimensional changes within the interferometer, and interferometer type, have on the photodetector output. A large array is used to store a time domain sequence of the angle modulated laser output. Each array point is a time slice of the modulated waveform. The array length is chosen to be exactly 2^n long and we adjust the time slice such that exactly a whole number of carrier cycles and modulation cycles fit it. This arrangement can now be used as a circular buffer, as the beginning and end match up. For example, with a laser wavelength of 830 nm (361 THz), a modulating signal of 10 GHz and a buffer size of 4,194,304 we can fit 8 modulation cycles, with each carrier cycle sampled 14.52 times. Because the ends of the array match up, we do not need a windowing function and the Fourier transform is an ideal case, offering very low noise.

A Michelson interferometer may be modeled by moving through the array with two pointers, one offset by the path length delay from the other. The contents addressed by the two pointers are added together and stored in another array. A Fabry-Perot interferometer simulation uses multiple taps with a weighting factor appropriate to the reflection and finesse of the cavity. The circular buffer is essential in this mode, as one may use hundreds of taps. A square law detector may be modeled by simply squaring the contents of each array element. The model generates an output that is rich in phase, amplitude, power, time domain, and frequency domain information.

Experimental Results

An experiment was performed to verify the operation of the interferometric comb generator. The system parameters were:

- a) Laser drive current 200 mA
- b) Average output power of interferometer 8 mW
- c) Microwave modulation frequency 2.154 GHz
- d) Available microwave modulation power 16.8 dBm
- e) Interferometer path length difference 14 cm

The New Focus 1434 photodetector has a nominal operating bandwidth of 25 GHz. Its output port is a SMA connector. The microwave comb output up to 26 GHz was observed directly with a spectrum analyzer. Between 26 and 46 GHz we connect a WR-28/K-connector transition to the photodetector. A HP 1197Q waveguide harmonic mixer was used as an external mixer for the spectrum analyzer. Because the photodetector's output is above the frequency limit of its SMA connector, power coupling is expected to drop above 32 GHz. As well, above 40 GHz, the efficiency of the harmonic mixer and the waveguide transition rolls off rapidly. For frequencies greater than 50 GHz, a K to V adapter, followed by a V-connector/WR-15 waveguide transition, and a Pacific Millimeter WR-10 harmonic mixer were connected to the spectrum analyzer as an external mixer. The power measurement was not calibrated in this frequency range. The noise floor of the power measurements ranged from -102 dBm to -110 dBm.

The output frequencies were all found at multiples of the microwave pump. From the pattern of the output power, we determined that 98% of the power in the comb is contained below about 40 GHz. This suggests that the angle modulation of the laser had a modulation index (β) of about 10. Figure 2 is a graph of the comb power versus frequency. Figure 3.a is the predicted response produced by the numerical model. Figure 3.b is the frequency modulated optical input signal to the interferometer as given by the numerical model.

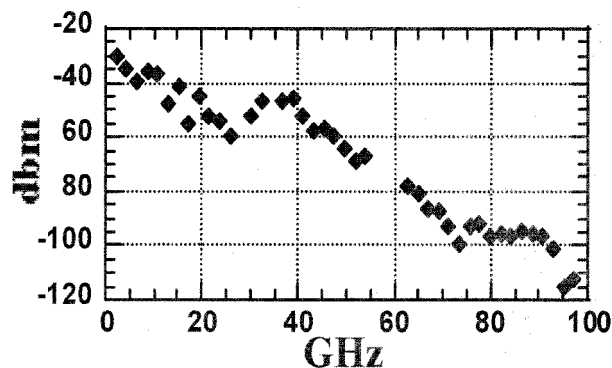


Figure 2. Graph of the microwave comb line power measured by the spectrum analyzer vs the frequency of the comb line. X-axis is frequency in GHz and Y-axis is power in dBm.

Both the numerical and experimental data sets display a similar sharp roll-off pattern above 40 GHz. We conclude that there is qualitative agreement between the numerical model and the experimental results. With one arm of the interferometer removed the output power dropped as much as -37 dB at 53.85 GHz, the highest frequency for which this effect was measured. The reduction in output power with one arm of the interferometer removed is less at lower frequencies due to gain switching of the laser. Gain switching is a nonlinear response of the amplitude of the laser to changes of the input current. Figure 4 is the spectrum of a comb line at 15.078 GHz (7th harmonic).

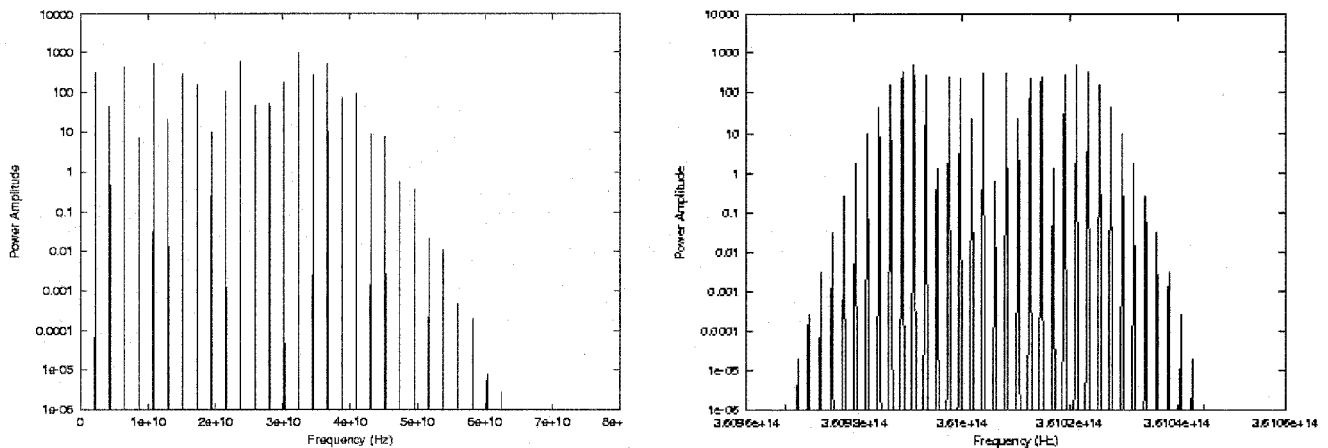


Figure 3. a) Numerical model prediction of comb output
b) Numerical model prediction of optical input to the interferometer

In a subsequent experiment we measured the increase of phase noise of the photodetector's output as a function of harmonic number. The ratio of phase noise power to carrier power of a given line in the photodetector's output should be n^2 , where n is the harmonic number of the output line. The laser was modulated with a 100 MHz signal which was itself frequency modulated at 50 kHz to produce a pair of discrete sidebands. The interferometer output was therefore a comb of lines spaced at 100 MHz intervals, and each line had 50 kHz sidebands. The ratio of the power in the comb line and its associated sideband at 50 kHz offset was measured from 100 MHz to 1.8 GHz, the 17th harmonic of 100 MHz, at the output of the photodetector. The excess phase noise (above the n^2 ratio) ranged from 0.5 dB at 300 MHz to 5 dB at 1.8 GHz.

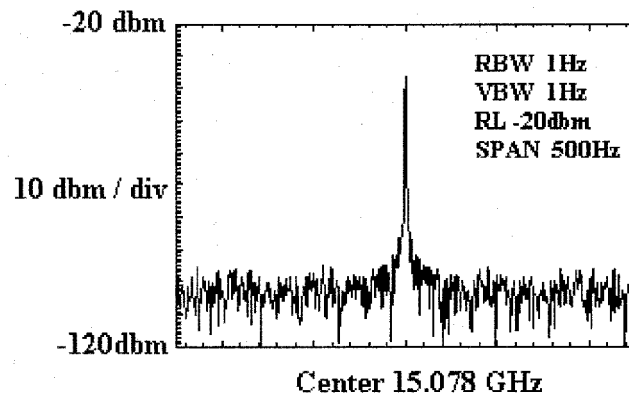


Figure 4. Spectrum of one of the comb lines

A third experiment was done to determine if the output was phase stable with respect to the modulating signal ω_m . The modulating signal was split with half going to the laser and the other half going to the input of a frequency multiplier. The output of the frequency multiplier was the same frequency as the comb line to be phase compared. The two frequencies after down conversion to 70MHz were inputs to a HP8508A vector voltmeter, with the frequency multiplier's output acting as the reference. Lines at 8.616 GHz and 17.232 GHz were examined. Over a 10 minutes time scale, measurements were taken. The 8.616 line was phase stable to about 1 degree rms, while the 17.232 GHz line had a short term stability of about 2 degrees rms with a drift of about 2 degrees. One degree at 17.232 GHz corresponds to about 48 microns in free space so some of the measured drift may be caused by the collection of cable and devices required for the test. For longer time scales the polarization stability of our interferometer became the limiting factor.

Conclusion

A simple photonic microwave comb generator has been demonstrated and mathematically modeled. The generality of the approach suggests that other means of producing an angle modulated output, and other types of interferometers, may be used to build better devices with higher power output to higher frequencies. Photodetectors are currently commercially available with a DC to 60 GHz frequency response. However, photodetectors with response to several hundred GHz are available in some laboratories. Furthermore, Phase modulators are available with a DC to 40 GHz frequency response and a V_π of 6 Volts (π radians of phase shift with 6 Vrms input). Polarization preserving fiber couplers are also available. Given the interest in solid state local oscillators for heterodyne applications, it seems likely that our type of frequency generation scheme will be used throughout the submillimeter in the near future.

References

1. T. Noguchi, A. Ueda, H. Iwashita, S. Takano, Y. Ishibashi, H. Ito, and T. Nagatsuma "Millimeter Wave Generation Using a Uni-Traveling-Carrier Photodiode" Proceedings of the Twelfth International Symposium on Space Terahertz Technology (2001)
2. P.G. Huggard, B.N. Ellison, P. Shen, N.J. Gomes, P.A. Davies, W.P. Shillue, A. Vaccari, W. Grammer, and J.M. Payne "A Photonic MM-Wave Reference and Local Oscillator Source" Alma Memo #396
3. S. Verghese, E.K. Duerr, K.A. Mcintosh, S.M. Duffy, S.D. Calawa, C-Y.E. Tong, R. Kimberk, and R. Blundell "A Photomixer Local Oscillator For 630-GHz Heterodyne Receiver" IEEE Microw. Guid. Wave Lett. 9, 245 (1999)
4. J. M. Payne L.D. Addario, D.T. Emerson, A.R. Kerr, B. Shillue "Photonic local oscillator for the Millimeter Array" SPIE Vol. 3357
5. Ferrel G. Stremler "Introduction to Communication Systems" third edition Addison-Wesley Publishing Company
6. T. Bosch, S. Pavageau, D. d'Alessandro, N. Servagent, V. Annovazzi-Lodi, and S. Donti "A low-cost, optical feedback laser range-finder with chirp-control" IEEE Instrumentation and Measurement Technology Conference Budapest, Hungary, May 21-23, 2001
7. Chung E.Lee, William N. Gibler, Robert A. Atkins, and Henry F. Taylor "In-Line Fiber Fabry-Perot Interferometer with high-Reflectance Internal Mirrors" Journal of Lightwave Technology, Vol. 10, No. 10, October 1992
8. Ana Garcia Armada "Understanding the Effects of Phase Noise in Orthogonal Frequency Division Multiplexing (OFDM)" IEEE Transactions On Broadcasting, Vol. 47, NO. 2, June 2001 Pallab Bhattacharya "Semiconductor Optoelectronic Devices" second edition Prentice hall 1997 page 268.